Quantum size effects on excitonic Coulomb and exchange energies in finite-barrier semiconductor quantum dots

J. M. Ferreyra and C. R. Proetto
Comisión Nacional de Energía Atómica, Centro Atómico Bariloche and Instituto Balseiro, 8400 Bariloche, Argentina
(Received 19 February 1998: revised manuscript received 2 November 1998)

The size dependence of the one-particle band gap and the Coulomb and exchange excitonic corrections of spherical quantum dots are calculated using the effective-mass approximation with finite confining potentials. Full analytical expressions are found for the three magnitudes, and it is shown that the Coulomb and exchange excitonic corrections are in good qualitative and quantitative agreement with available state-of-the-art calculations (for Si, GaAs, and CdSe) and experiments (for InP). [S0163-1829(99)16435-X]

The experimental and theoretical study of quantum size effects in quantum dot (QD) semiconductor heterostructures has become a very active research area, both because of their unique physical properties and prospect for applications.[1] As the size of the QD is reduced, both the single-particle band gap increases (blueshift) and the electron-hole excitonic correction becomes more pronounced (redshift). However, as the size dependence of the former is usually stronger than the exciton size dependence, this results in an overall blueshift of the optical-absorption spectrum (as compared with the bulk). Additional impulse to these studies was provided by the discovery of visible luminescence from porous Si.[2] Although the microscopic mechanism, which is behind the photoluminescence, is still under debate, there exists a growing consensus that quantum confinement is involved in producing this phenomenon.[3]

From the theoretical point of view, the electronic structure of small quantum dots has been studied by a variety of methods: single-band effective-mass approximation (EMA),[4] multiband effective-mass approximation with infinite confining barriers,[5] empirical tight-binding (ETB),[6] empirical pseudopotential method (EPM),[7] and *ab initio* pseudopotential calculations.[8] There is a tendency to disregard the EMA as a quantitative and even qualitative method for the study of these nanocrystallites, mainly because the comparison of the EMA with the latter more sophisticated and reliable techniques shows large discrepancies, as, for instance, a gross EMA overestimation of the one-particle band gap. This is an important issue, as the great advantage of the EMA is its flexibility and versatility, in addition to allowing a quite natural extension to situations with electric and magnetic external fields, the presence of impurities, etc.[9] A point worth noting is that most often [i.e., Refs. 6(c), 6(d), 7, and 8] EMA is associated with the infinite barrier approximation for the quantum dot confining barrier (IEMA); this is clearly the simplest version of the EMA, but obviously the less accurate. It is the aim of this work to demonstrate that just by relaxing this hard-wall boundary condition, the finite barrier version of the EMA (FEMA) gives quantum size effects for Coulomb and exchange exciton energies in quite good agreement with the more accurate calculations available to date.

Using the envelope function approach to the effective-mass approximation, the Hamiltonian of the electron-hole system in a spherical dot[10] of radius a is given by

$$H = H_e + H_h + H_{e\text{-}h}, \tag{1}$$

where $H_i = -\hbar^2 \boldsymbol{\nabla} 1/2m_i(r_i)\boldsymbol{\nabla} + V_i(r_i)$ is the single-particle Hamiltonian $(i=e,h)$, and $H_{e\text{-}h} = -e^2/\varepsilon|\mathbf{r}_e - \mathbf{r}_h|$ is the electron-hole Coulomb attraction. $V_e(r_e)$ and $V_h(r_h)$ are the electron and hole-confining potentials, respectively, defined as $V_i(r_i)=0$ if $r_i < a$ and $V_i(r_i)=V_{i2}$ if $r_i > a$. Here, $m_i(r_i)$ is the particle effective mass, with values m_{i1} (m_{i2}) inside (outside) the quantum dot, and ε is the dielectric constant of the well-acting semiconductor.[11] As the exact solution of Eq. (1) is not known, even in the simplest situation $V_{i2} \to \infty$, we should resort to some approximate treatment. Keeping in mind that most of the above quoted calculations are restricted to sizes $d=2a$ small compared with the exciton Bohr-radius a_{ex} ($a_{\mathrm{ex}} \simeq 5$ nm for bulk Si), we will employ the so-called strong-confinement approximation (SCA),[12] which amounts to consider the electron-hole Coulomb interaction as a small perturbation against the single-particle terms.[13] The approximation, that is asymptotically exact in the $a/a_{\mathrm{ex}} \ll 1$ limit, has also been employed in Refs. 5–8 [the single exception being the ETB calculation of Ref. 6(d)] and applied to study the problem of doping QD's with impurities.[14] Accordingly, we will concentrate first on the one-particle solutions of H_i.

Proposing a separable solution $\phi_{lm}(\mathbf{r}_i) = R_l(r_i) Y_{lm}(\theta_i, \varphi_i)$ and taking $l=m=0$ (ground state), the solutions of $H_i \phi_{00}(\mathbf{r}_i) = E_i \phi_{00}(\mathbf{r}_i)$ are given by $\phi_{00}(\mathbf{r}_i) = R_0(r_i)/\sqrt{4\pi}$, where $R_0(r_i) = A_i \sin(\alpha_i r_i)/r_i$ if $r_i < a$, while $R_0(r_i) = B_i e^{-\beta_i r_i}/r_i$ if $r_i > a$. A_i and B_i are normalization constants, while $\alpha_i = (2m_{i1}E_i/\hbar^2)^{1/2}$ and $\beta_i = [2m_{i1}(V_{i2} - E_i)/\hbar^2]^{1/2}$. From the Daniel-Duke boundary conditions[9] $R_0(a^-) = R_0(a^+)$ and $R_0'(a^-)/m_{i1} = R_0'(a^+)/m_{i2}$, we obtain the implicit eigenvalue equation[4]

$$(\alpha_i d/2)\cot(\alpha_i d/2) = 1 - \frac{m_{i1}}{m_{i2}} - \frac{m_{i1}}{m_{i2}}(\beta_i d/2). \tag{2}$$

The size-dependent one-particle band gap is defined as $E_g(d) \equiv E_g(\infty) + E_e(d) + E_h(d)$, where $E_g(\infty)$ is the one-particle band gap of the semiconductor QD bulk material, and $E_e(d)$, $E_h(d)$ are the size-dependent solutions of Eq. (2), with $i=e,h$, respectively.

In the limit $E_i/V_{i2} \ll 1$, we obtain an analytical expression for the size-dependent gap

TABLE I. Electronic parameters for the indicated crystalline materials.

	$m_{e1}(m_0)$	$m_{h1}(m_0)$	V_{e2} (eV)	J(meV)
Si	0.26 [a]	0.23 [a]	4 [b]	0.15 [c]
GaAs	0.07 [a]	0.68 [a]	4 [b]	0.03 [d]
InP	0.073 [e]	0.4 [e]	4 [b]	
CdSe	0.13	0.45	4.4 [b]	

[a]Reference 19.
[b]Reference 20.
[c]Reference 15.
[d]Reference 16.
[e]Reference 4.

$$E_g(d)=E_g(\infty)+\frac{\hbar^2}{2\mu}\left(\frac{2\pi}{d}\right)^2-E_e^\infty\delta_e-E_h^\infty\delta_h+\mathcal{O}(V_{i2}^{-1}), \quad (3)$$

where $\mu=m_{e1}m_{h1}/(m_{e1}+m_{h1})$ is the exciton reduced mass of the QD semiconductor, $E_i^\infty=(2\pi\hbar/d)^2/2m_{i1}$ are the electron and hole solutions of Eq. (2) with V_{e2}, $V_{h2}\rightarrow\infty$, and $\delta_i=\sqrt{8m_{i2}\hbar^2/m_{i1}^2d^2V_{i2}}$. In addition to its relative utility for quantitative estimations (see below), Eq. (3) is, however, quite useful to obtain a qualitative understanding on the influence of the system parameters on $E_g(d)$. For instance, taking $V_{i2}\rightarrow\infty$, we recover the d^{-2} scaling for the size-dependent one-particle band gap, frequently quoted as a gross failure of the EMA. This is corrected, however, by the third and fourth terms in Eq. (3), which, being negative and scaling as d^{-3}, lead to a softer dependence of $E_g(d)$ on d of the type $d^{-\gamma}$ (with γ typically between 1 and 2). It is also interesting to realize that for a constant value of the confining barriers the correction increases by decreasing d and also if the effective mass of the particle in the surrounding medium is larger than inside the QD.

Next, and following the spirit of the SCA, we have calculated the Coulomb excitonic contribution, by taking the matrix element of $H_{e\text{-}h}$ with the uncorrelated excitonic state $\Psi_{\mathrm{ex}}(\mathbf{r}_e,\mathbf{r}_h)\equiv\phi_{00}(\mathbf{r}_e)\phi_{00}(\mathbf{r}_h)$ of our FEMA. We define

$$\begin{aligned}E_{\mathrm{Coul}}(d)&\equiv-\langle\Psi_{\mathrm{ex}}(\mathbf{r}_e,\mathbf{r}_h)|H_{e\text{-}h}|\Psi_{\mathrm{ex}}(\mathbf{r}_e,\mathbf{r}_h)\rangle\\&=(e^2/\varepsilon)(I_1+I_2+I_3)\end{aligned} \quad (4)$$

with

$$I_1=\frac{A_e^2A_h^2d}{8}\left\{1-\frac{\sin\alpha_e'}{\alpha_e'}-\frac{\mathrm{Si}\,\alpha_e'}{\alpha_e'}+\frac{1}{2\alpha_e'}\times[\mathrm{Si}(\alpha_e'-\alpha_h')+\mathrm{Si}(\alpha_e'+\alpha_h')]\right\}+e\rightleftarrows h, \quad (5)$$

$$I_2=\frac{A_e^2B_h^2d}{4}\left(1-\frac{\sin\alpha_e'}{\alpha_e'}\right)\mathrm{E}_1(\beta_h')+e\rightleftarrows h, \quad (6)$$

$$I_3=\frac{B_e^2B_h^2d}{2\beta_e'}[e^{-\beta_e'}\mathrm{E}_1(\beta_h')-\mathrm{E}_1(\beta_e'+\beta_h')]+e\rightleftarrows h, \quad (7)$$

where $\alpha_i'=\alpha_id$, $\beta_i'=\beta_id$, and $\mathrm{Si}(x)$ and $\mathrm{E}_n(x)$ are the sine and exponential integral functions, respectively. All three contributions to $E_{\mathrm{Coul}}(d)$ have a transparent physical interpretation: I_1 (I_3) corresponds to a situation where both electron and hole are inside (outside) the QD, while I_2 corresponds to a situation with one particle inside the dot and the second particle outside. In typical situations ($d\gtrsim1$ nm), both I_2 and I_3 are 2–3 orders of magnitude smaller than I_1. Expanding Eqs. (5)–(7) around the hard-wall limit, we obtain the asymptotic expression

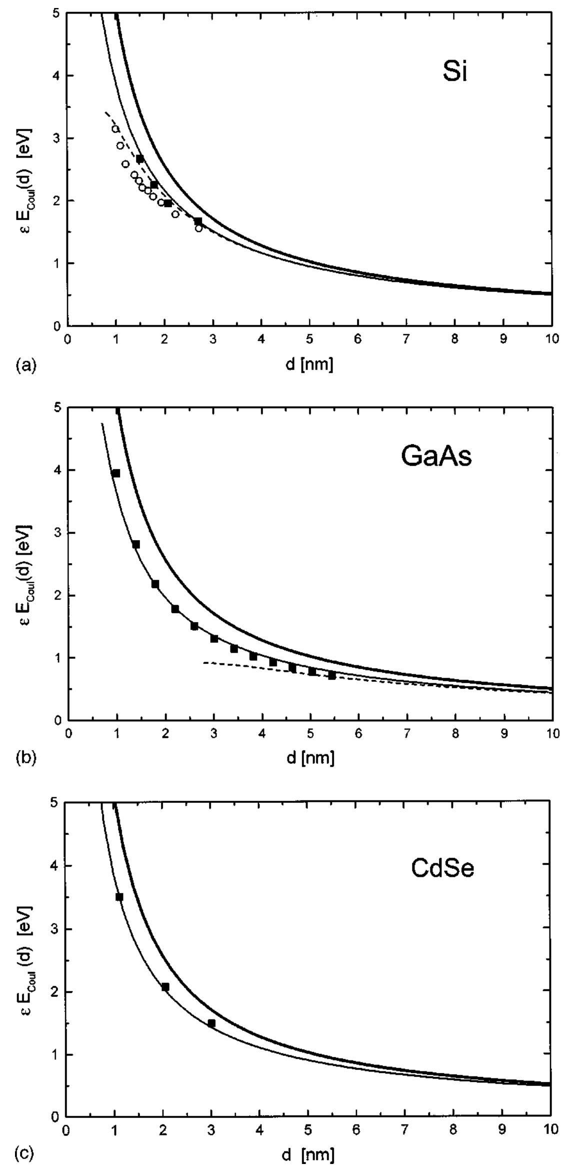

FIG. 1. Unscreened Si (a), GaAs (b), and CdSe (c) exciton Coulomb energies as a function of the quantum dot diameter d. Thick line, IEMA; thin line, FEMA; dashed line, FEMA (asymptotic). Solid squares, EPM [Ref. 7(b)]; open circles, *ab initio* pseudopotential method (Ref. 8).

$$E_{\mathrm{Coul}}(d)=E_{\mathrm{Coul}}^\infty(d)[1-(\delta_e+\delta_h)/4]+\mathcal{O}(V_{i2}^{-1}), \quad (8)$$

where $E_{\mathrm{Coul}}^\infty(d)=4e^2[1-\mathrm{Si}(2\pi)/2\pi+\mathrm{Si}(4\pi)/4\pi]/\varepsilon d\simeq3.572e^2/\varepsilon d$ is the corresponding result for infinite confining barriers, as obtained by Brus.[13] Similarly to the situation for the size dependence of the one-particle band gap, the ''universal'' scaling of the type d^{-1} of $E_{\mathrm{Coul}}^\infty(d)$ is modified by the finite barrier correction, which being negative and scaling as d^{-2} leads to a softer size dependence of $E_{\mathrm{Coul}}(d)$.

Another interesting QD size effect is the enhancement of the electron-hole exchange interaction, which gives the en-

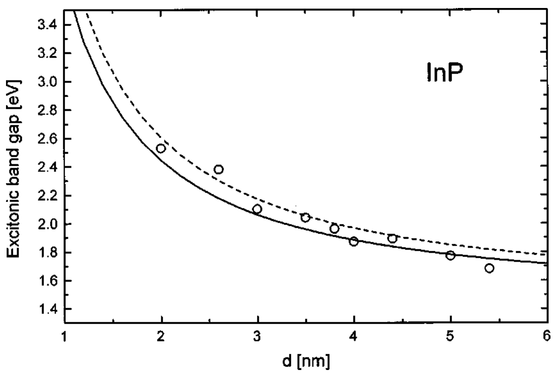

FIG. 2. Single-particle and excitonic band gaps for InP quantum dots of different sizes. Open circles, experimental excitonic band gap from Ref. 22; dashed line, single-particle band gap $E_g(d)$ [eV] $=1.45+37.295/d$ [A]$^{1.16}$ from Ref. 23; solid line, calculated excitonic band gap $E_g(d)-E_{\text{Coul}}(d)$.

ergy difference between spin-singlet and spin-triplet excitons. Although being only a fraction of meV in bulk Si (Ref. 15) and GaAs,[16] it could reach a few meV in Si nanocrystals, porous Si, and GaAs QD's because of the strong confinement. We define[17,18]

$$E_{\text{exch}}(d)\equiv \pi a_{\text{ex}}^3 J\int d\mathbf{r}|\Psi_{\text{ex}}(\mathbf{r},\mathbf{r})|^2, \tag{9}$$

where J is the exchange energy of the $1s$ bulk exciton. Using for the calculation of $E_{\text{Coul}}(d)$ the uncorrelated excitonic state, we obtain the analytic expression

$$E_{\text{exch}}(d)=(a_{\text{ex}}^3 J/4)(J_1+J_2), \tag{10}$$

where

$$J_1=\frac{A_e^2A_h^2}{d}\left\{-\sin^2\left(\frac{\alpha_e'}{2}\right)\sin^2\left(\frac{\alpha_h'}{2}\right)+\frac{\alpha_e'}{2}\text{Si}(\alpha_e')-\frac{\alpha_e'}{4}\right.$$
$$\left.\times[\text{Si}(\alpha_e'-\alpha_h')+\text{Si}(\alpha_e'+\alpha_h')]\right\}+e\rightleftarrows h, \tag{11}$$

$$J_2=(2B_e^2B_h^2/d)\text{E}_2(\beta_e'+\beta_h'). \tag{12}$$

Expansion of Eqs. (11) and (12) around the infinite barrier limit, yields the asymptotic approximation

$$E_{\text{exch}}(d)=E_{\text{exch}}^{\infty}(d)[1-3(\delta_e+\delta_h)/4]+\mathcal{O}(V_{i2}^{-1}), \tag{13}$$

where $E_{\text{exch}}^{\infty}(d)=\pi[\text{Si}(2\pi)-\text{Si}(4\pi)/2]J(2a_{\text{ex}}/d)^3 \simeq 2.111J(2a_{\text{ex}}/d)^3$.[17] Comparison of the asymptotic expressions (3), (8), and (13) reveals that in all cases the leading correction to the IEMA can be described in terms of the dimensionless parameters δ_e and δ_h.

For the quantitative evaluation of $E_g(d)$, $E_{\text{Coul}}(d)$, and $E_{\text{exch}}(d)$, we use the material parameters given in Table I.[21] In addition, assuming that the QD's are in vacuum, we adopt $m_{e2}=m_{h2}=m_0$, V_{e2} as given by the electron affinity of the corresponding bulk material, and $V_{h2}\to\infty$. Equipped with these *bulk* (that is, not adjustable) parameters, we evaluate $E_g(d)$, $E_{\text{Coul}}(d)$, and $E_{\text{exch}}(d)$; the results for the excitonic properties are displayed in Figs. 1–3.

As expected, our results for $E_g(d)$ (not shown), although well below the infinite barrier results, still lie above the more accurate results obtained from ETB or EPM calculations. As discussed above, both the use of finite barriers and the fact

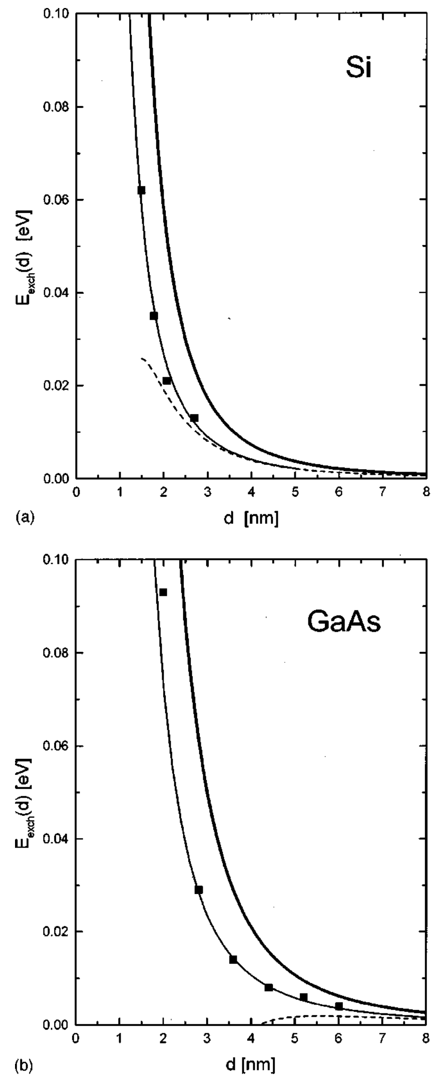

FIG. 3. Electron-hole Si and GaAs exchange interaction as a function of the quantum dot diameter *d*. Same convention as in Fig. 1.

that the electron and hole effective masses in vacuum are larger than inside the QD contributes in the right direction by decreasing the one-particle band gap, but still the effects are not large enough to lead our FEMA results in good agreement with more accurate calculations. The discrepancy increases as dot size decreases: defining $\Delta E_g(d)\equiv[E_g^{\text{FEMA}}(d)-E_g^{\text{EPM}}(d)]/E_g^{\text{EPM}}(d)$, we obtain $\Delta E_g(4\ \text{nm})\simeq 5\%$, while $\Delta E_g(2.5\ \text{nm})\simeq 21\%$, both for Si; replacing $E_g^{\text{FEMA}}(d)$ with $E_g^{\text{IEMA}}(d)$ we obtain for $\Delta E_g(4\ \text{nm})\simeq 12\%$ and $\Delta E_g(2.5\ \text{nm})\simeq 40\%$. On the other side and as we will see in what follows, this being the main point of this contribution, excitonic energies being less sensitive to the details of the QD electronic structure are quite well described by the FEMA (but not by the IEMA).

We have collected in Fig. 1 the results from different calculations for the unscreened Coulomb interaction $\varepsilon E_{\text{Coul}}(d)$ for Si, GaAs, and CdSe QD's. The softening allowed above is readily seen from this figure, with the effect being quite important in the small size limit. For Si, the comparison with the empirical and *ab initio* pseudopotential calculations of Refs. 7(c) and 8 is quite encouraging, the agreement being better with the empirical results. We give the corresponding results for GaAs and CdSe QD's in the middle and lower panels, respectively. The agreement with the EPM results is even better than for Si QD's. As an example of the practical use of FEMA, we provide in Fig. 2 a comparison between experimental and theoretical excitonic band gaps for InP dots of different sizes. To correct the above discussed failure of FEMA in reproducing the size-dependent single-particle band gap, we propose to take $E_g(d)$ from a more microscopic approach[6–8] and correcting it with $E_{\rm Coul}(d)$ as given by FEMA. As can be seen from Fig. 2, proceeding in this way, we obtain good agreement between experimental and calculated excitonic band gaps.[11]

We collect all the results for $E_{\rm exch}(d)$ in Si QD's in the upper panel of Fig. 3. Once more, FEMA leads to a size dependence for $E_{\rm exch}(d)$ slower than the d^{-3} hard-wall scaling. Even so, the excitonic exchange interaction in QD's can easily be enhanced in 2 orders of magnitude over the bulk value by quantum confinement, remaining however much smaller than $E_{\rm Coul}(d)$. The lower panel of Fig. 3 corresponds to $E_{\rm exch}(d)$ for GaAs QD's. In addition to the overall remarkable agreement between FEMA and EPM calculations displayed in Fig. 3, it is interesting to note that while in bulk the energy difference between spin-singlet and spin-triplet excitons is much larger in Si than in GaAs $[J(\mathrm{Si})/J(\mathrm{GaAs}) \simeq 5]$ the situation is the opposite in the strong-confinement regime. The explanation is quite natural from Eq. (9), as the parameter that matters in this regime for $E_{\rm exch}$ is $J\,a_{\rm ex}^3$; as $a_{\rm ex}(\mathrm{GaAs}) \gg a_{\rm ex}(\mathrm{Si})$, this more than compensates for the fact that the bulk exchange excitonic splitting is much smaller in GaAs as compared with Si.

In summary, we have included two simple but realistic effects in the EMA: the finite height of the confining QD barriers and the difference between electron and hole effective masses inside and outside the QD. Contrary to the somehow widespread belief, these modifications bring the FEMA results on the Coulomb and exchange excitonic energies of semiconductor QD's in close agreement with full numerical state-of-the-art calculations, mainly smaller energies and softer power-law dependence on dot sizes for both corrections, as compared with IEMA. Based on this success, enhanced by the fact that we have no adjustable parameters in our theory, we believe that FEMA can be quite useful as a complementary tool for the more accurate calculations of QD, for example, by extending these calculations to dot sizes where they are not available ($d \gtrsim 3$ nm).

One of us (J.M.F.) is indebted to CONICET of Argentina for financial support at the starting stage of this project; the authors thank Pablo Bolcatto for help with the numerical calculations and Karen Hallberg for a careful reading of the manuscript.

[1] (a) A. D. Yoffe, Adv. Phys. **42**, 173 (1993); (b) L. Banyai and S. W. Koch, *Semiconductor Quantum Dots* (World Scientific, Singapore, 1993); (c) U. Woggon and S. V. Gaponenko, Phys. Status Solidi B **189**, 285 (1995).

[2] L. T. Canham, Appl. Phys. Lett. **57**, 1046 (1990).

[3] D. J. Lockwood, Solid State Commun. **92**, 101 (1994).

[4] L. E. Brus, J. Chem. Phys. **79**, 5566 (1983).

[5] (a) T. Takagahara and K. Takeda, Phys. Rev. B **46**, 15 578 (1992); (b) **53**, R4205 (1996).

[6] (a) P. E. Lippens and M. Lannoo, Phys. Rev. B **39**, 10 935 (1989); (b) J. P. Proot, C. Delerue, and G. Allan, Appl. Phys. Lett. **61**, 1948 (1992); (c) M. Lannoo *et al.*, Phys. Rev. Lett. **74**, 3415 (1995); (d) N. A. Hill and K. B. Whaley, *ibid.* **75**, 1130 (1995).

[7] (a) M. V. Rama Krishna and R. A. Friesner, Phys. Rev. Lett. **67**, 629 (1991); (b) L. W. Wang and A. Zunger, J. Phys. Chem. **98**, 2158 (1994); (c) A. Franceschetti and A. Zunger, Phys. Rev. Lett. **78**, 915 (1997).

[8] S. Öğüt *et al.*, Phys. Rev. Lett. **79**, 1770 (1997).

[9] G. Bastard, *Wave Mechanics Applied to Semiconductor Heterostructures* (Les Editions de Physique, Les Ulis, 1988).

[10] P. G. Bolcatto and C. R. Proetto, Phys. Rev. B **59**, 12 487 (1999). We demonstrate here that shape effects are quite small on Coulomb excitonic energies, even in the presence of sizable boundary dielectric mismatch.

[11] In a forthcoming contribution we analyze the effects related to the boundary dielectric mismatch *and* finite confinement barriers. These so-called dielectric confinement effects are known to be important in semiconductor quantum dots. They are not needed for the comparison of our (unscreened) results with state-of-art (unscreened) calculations of Figs. 1 and 3. Inclusion of image charge effects within IEMA gives an upward shift of the full line in Fig. 2 of a few tens of meV (~ 0.04 eV for $d = 40$ nm).

[12] Al. L. Efros and A. L. Efros, Phys. Tek. Poluprovodn. **16**, 1209 (1982) [Sov. Phys. Semicond. **16**, 772 (1982)].

[13] L. E. Brus, J. Chem. Phys. **80**, 4403 (1984).

[14] J. M. Ferreyra and C. R. Proetto, Phys. Rev. B **52**, R2309 (1996); C. R. Proetto, Phys. Rev. Lett. **76**, 2824 (1996).

[15] J. C. Merle *et al.*, Phys. Rev. B **17**, 4821 (1978).

[16] W. Ekardt *et al.*, Phys. Rev. B **20**, 3303 (1979).

[17] T. Takagahara, Phys. Rev. B **47**, 4569 (1993).

[18] G. Fishman *et al.*, J. Phys. IV **C5**, 355 (1993).

[19] W. F. Brinkman and T. M. Rice, Phys. Rev. B **7**, 1508 (1973).

[20] M. Cardona and L. Ley, *Photoemission in Solids I* (Springer, Berlin, 1978), Chap. 1.

[21] As a (partial) validation of our single-band approach, we have obtained the value of μ, the exciton reduced mass of Eq. (3), by fitting the infinite barrier multiband calculation of the size-dependent one-particle band gap for Si spherical quantum dots of Ref. 5(a) to $(2\pi\hbar/d)^2/2\mu$. Quite surprisingly, the fitting works nicely, producing $\mu \simeq (0.114 \pm 0.001)m_0$ (m_0 being the bare electron mass). This value of μ is quite close to $\mu(\mathrm{Si}) \simeq 0.12 m_0$ used in our single-band approach.

[22] O. I. Micic *et al.*, J. Phys. Chem. **98**, 4966 (1994); Appl. Phys. Lett. **68**, 3150 (1996).

[23] H. Fu and A. Zunger, Phys. Rev. B **55**, 1642 (1997).